2024 IEEE/RSJ International Conference on Intelligent Robots and Systems (IROS)
October 14-18, 2024. Abu Dhabi, UAE

Design of Upper-Limb Exoskeleton with Distal Branching Link Mechanism for Bilateral Operation of Humanoid Robots

Hiroki Yoshioka[1] , Naoki Hiraoka[1], Kunio Kojima[1], Kei Okada[1] and Masayuki Inaba[1]

***Abstract*— Exoskeletons for robot operation necessitate shoulders with high range of motions and high degrees of freedom to fit the operator's shoulder girdle. These shoulder joints need high torque for force feedback on the operator. Existing exoskeletons struggle to simultaneously meet these requirements of high DOFs, wide ROM, and high torque due to spatial constraints. This study introduces an exoskeleton with a distal branching link mechanism that addresses this issue by concentrating on each link's absolute and relative degrees of freedom. In the proposed exoskeleton, the end-effector's absolute DOF, the forearm's absolute DOF, and the end-effector and forearm's relative DOF are matched between the operator and the exoskeleton. This is achieved while reducing the overall DOF by sharing the root link system's DOF. Furthermore, by avoiding direct attachment of the operator to the exoskeleton's shoulder, the design can accommodate the human shoulder's high torque and high ROM. The study demonstrates that the branching exoskeleton outperforms existing link-fixed exoskeletons in terms of tracking the operator's arms and the torque required by the exoskeleton's joints. Utilizing this exoskeleton, we successfully maneuvered an actual humanoid robot to perform daily activities where the forearm posture is crucial.**

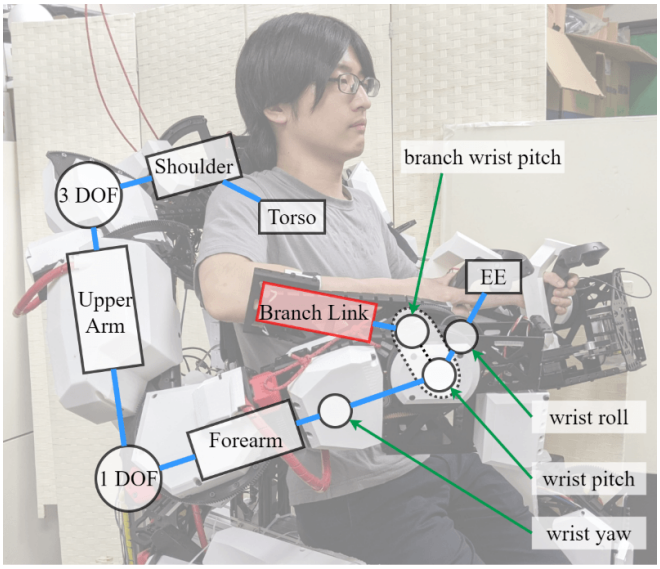

Fig. 1. Branching exoskeleton with an operator

I. INTRODUCTION

Master-slave systems employing exoskeletons have been explored for operating humanoid robots as replacements of human workers[1]. These exoskeletons require shoulders with high torque and high degrees of freedom. The shoulder's function extends beyond supporting the operator's weight; it must also exert substantial force to enable the operator to perceive the external forces acting on the robot. The human shoulder has intricate range of motion due to the conbination of plane joints and ball-and-socket joints[2]. Consequently, the existing exoskeletons incorporate 2-DOFs for the scapula and 3-DOFs for the shoulder[3][4][5]. To preserve the operator's arm redundancy, the exoskeleton's shoulder must offer high DOFs and a broad ROM. Existing exoskeletons face challenges in meeting the dual requirements of high-torque joints and multi-degree-of-freedom shoulders.

Traditional exoskeletons fall into two categories, end-fixed type and link-fixed type, based on their attachment method to the operator. The end-fixed type connects only the exoskeleton's end-effectors to the operator, specializing in end-effector maneuvering. However, it doesn't allow for observing the operator's arm's redundant DOFs. Despite this, the exoskeleton's joint arrangement has few restrictions, allowing for easy placement of high-torque joints. The link-fixed type, on the other hand, constrains all links, not just the operator's end-effector, to the exoskeleton. While it enables complete acquisition of the operator's posture, achieving high torque and a wide shoulder joint motion range simultaneously is challenging due to joint arrangement restrictions. The exoskeleton must follow the human arm's exterior while maintaining joint rotation axis alignment between the exoskeleton and the operator. It is difficult for the link-fixed type exoskeleton to construct a drive-train and frame structure capable of withstanding high loads under these strict constraints.

In this study, we introduce an exoskeleton design that incorporates a distal branching mechanism. This design addresses the issues of absolute and relative degrees of freedom for each exoskeleton link. The exoskeleton is attached to the operator's end-effectors and forearms. The proposed exoskeleton shares the same degrees of freedom from the torso to the end-effector and from the torso to the forearm in the arm linkage system, extending to the wrist. It features a branching structure at the wrist joint with two end-effectors, one for the forearm and another for the hand. While reducing the total DOFs, the absolute DOFs of the end-effector, the forearm, and the relative DOFs between the end-effector and forearm are aligned between the operator and the exoskeleton. By avoiding direct attachment of the operator to the exoskeleton' s shoulder links, and by adding a link

[1]H. Yoshioka, N. Hiraoka, K. Kojima, K. Okada and M. Inaba are with Department of Mechano-Infomatics, The University of Tokyo, 7-3-1 Hongo, Bunkyo-ku, Tokyo 113-8656, Japan yoshioka at jsk.t.i.u-tokyo.ac.jp

at the wrist instead of the base, a high-torque, high-motion-range exoskeleton structure can be achieved. This structure can accommodate the shoulder's complex movements of the operator.

II. DESIGN DESCRIPTION

This chapter describes the characteristics of the branching exoskeleton and existing exoskeletons. Existing exoskeletons are typically classified into two types: end-fixed type and link-fixed type as shown in Fig. 3 and Fig. 4, based on how they are attached to the operator.

A. Branching Exoskeleton (proposed mechanism)

The branching type exoskeleton is specifically designed to be attached to the operator at two specific points: the end effector and the forearm. To achieve this, a 1-DOF "Branch Link" is incorporated at the wrist joint as shown in Fig. 2, branching in the opposite direction from the other links, extending from the end-effector to the root link. The forearm of the operator is then attached to this link. This exoskeleton encompasses several notable features:

- It has the capability to acquire the posture of the operator's forearm, thereby enabling the operator to effectively control the redundant degrees of freedom within the robot's arm.
- Due to the placement of the additional branching link on the end-effoctor side rather than the root link side, only a limited number of joints require high torque for operation.
- Both of the points that attach the operator possess more than 6DOFs originating from the torso, ensuring that they do not restrict the motion of the forearms.
- The total number of DOFs in this exoskeleton's arm is optimized to 8, representing the minimum requirement of DOFs.
- The relative DOFs between the end-effector and the branch link are 3DOFs, the same as the human wrist joint.

In the redundant DOFs operation of the arm, it is not necessary to attach all the links of the exoskeleton to the operator, but it is necessary to acquire the elbow position. In this study, among the upper arm and forearm, we chose to attach the forearm that is close to the end-effector. Since the operator is restrained at only two points, the internal force generated between the restraining points can be minimized. Given that the branch link fixing the operator's forearm is added to the end-effector side, the joint torque of the exoskeleton against the exerted force on the operator is considered smaller than that of the structure with an additional link on the root link side. Furthermore, the branched structure provides 6-DOFs and 3-DOFs relative to the torso and forearm, and forearm and end-effector, respectively. Although the mechanism has 8-DOFs in total, it can be said to be compatible with a human arm with 9-DOFs. The branching exoskeleton integrates characteristics from the existing exoskeletons described below.

B. End-fixed Type Exoskeleton

The end-fixed exoskeleton is attached to the operator only on the end-effector, as depicted in Fig. 3. Many exoskeletons of this category are derived from robotic arms[6][7]. Moreover, exoskeletons like TABLIS[8] and HERMES[9] have been devised to operate the robot's gait. Key characteristics of this exoskeleton type include:

- Inability to capture the forearm motion of the operator, thereby restricting redundant DOF movement of robots.
- High torque is essential only for three specific joints.
- Only 7-DOFs are necessary for executing all operations effectively.

This method is specialized for maneuvering end-effectors and offers 7-DOFs, unlike the 9-DOFs in the human arm. It is fundamentally impossible to control a robot with redundant DOFs. While it can accurately convey exerted force on the robot to the operator's hand, managing torque distribution across the operator's joints is not feasible. However, the robot

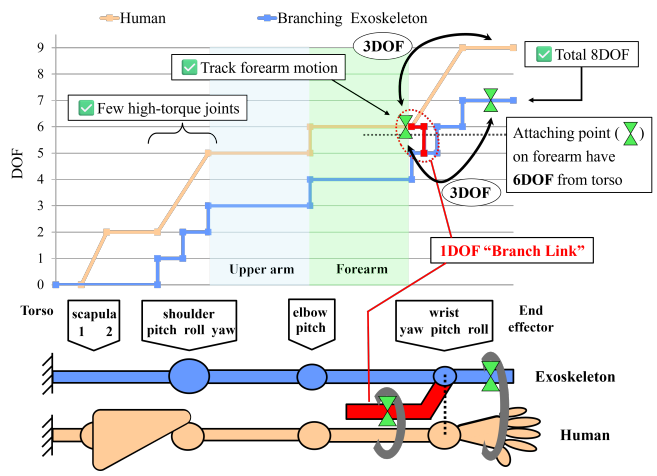

Fig. 2. The DOF arrangement and the attaching method of branching exoskeleton with 8-DOFs

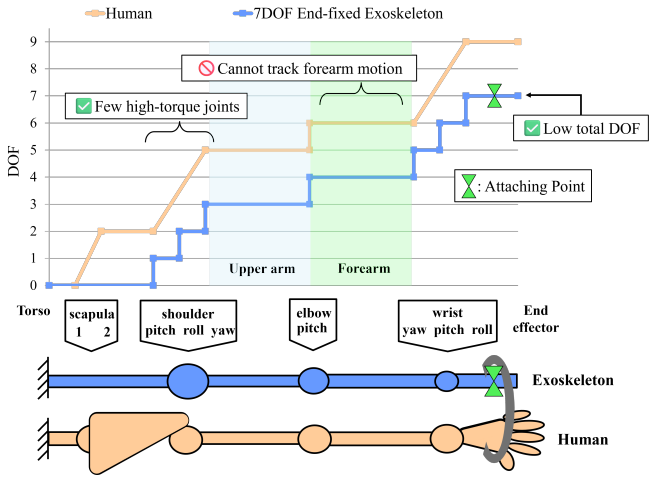

Fig. 3. The DOF arrangement and the attaching point of end-fixed type exoskeleton with 7-DOFs

arm features a simple structure with a mechanism akin to a standard robotic arm.

C. Link-fixed Type Exoskeleton

The link-fixed type exoskeleton is attached to the operator at three points: upper arm, forearm, and end-effector. This structure is depicted in Fig. 4. For instance, 7-DOF exoskeletons like ETS-MARSE[10], DE VITO[11], SAM[12], and SUEFUL-7[13] have been developed. However, these mechanisms are unable to accommodate 9-DOF movements, including those of the human shoulder-girdle. As a result, exoskeletons that have 9 or higher DOFs such as ANYexo[3], Harmony[4], IntelliArm[14] and KULEX[15] have been introduced. Furthermore, despite the total number of active DOFs not reaching 9 due to the exclusion of hand DOFs and the incorporation of passive joints, exoskeletons capable of mimicking human shoulder movements have been developed[5][16][17][18][19][20][21]. In contrast to the branching exoskeleton, these systems feature additional DOFs on the root link side. Key attributes of this exoskeleton type include:

- The operator's forearm and upper arm are attached to the exoskeleton, enabling the robot to maneuver with redundant degrees of freedom.
- Requirement for high torque at up to five joints.
- Necessity for 9 DOFs, aligning with the human arm's degree of freedom.

This method's exoskeleton can precisely capture the operator's movements, even redundant DOFs. The motors align coaxially with each of the operator's joints, enabling direct torque application to the joints. Nonetheless, due to multiple constraint points between the operator and the exoskeleton, internal forces arise at these points. Moreover, several joints on the root link side necessitate substantial torque, rendering the mechanism larger in comparison to a branching exoskeleton.

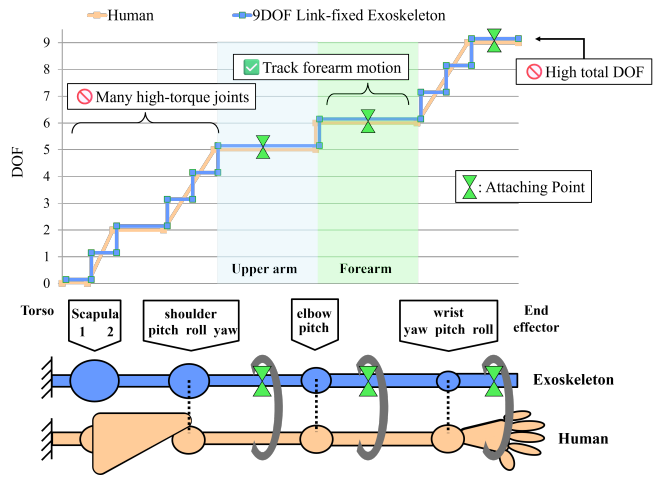

Fig. 4. The DOF arrangement and the attaching points of link-fixed type exoskeleton with 9-DOFs

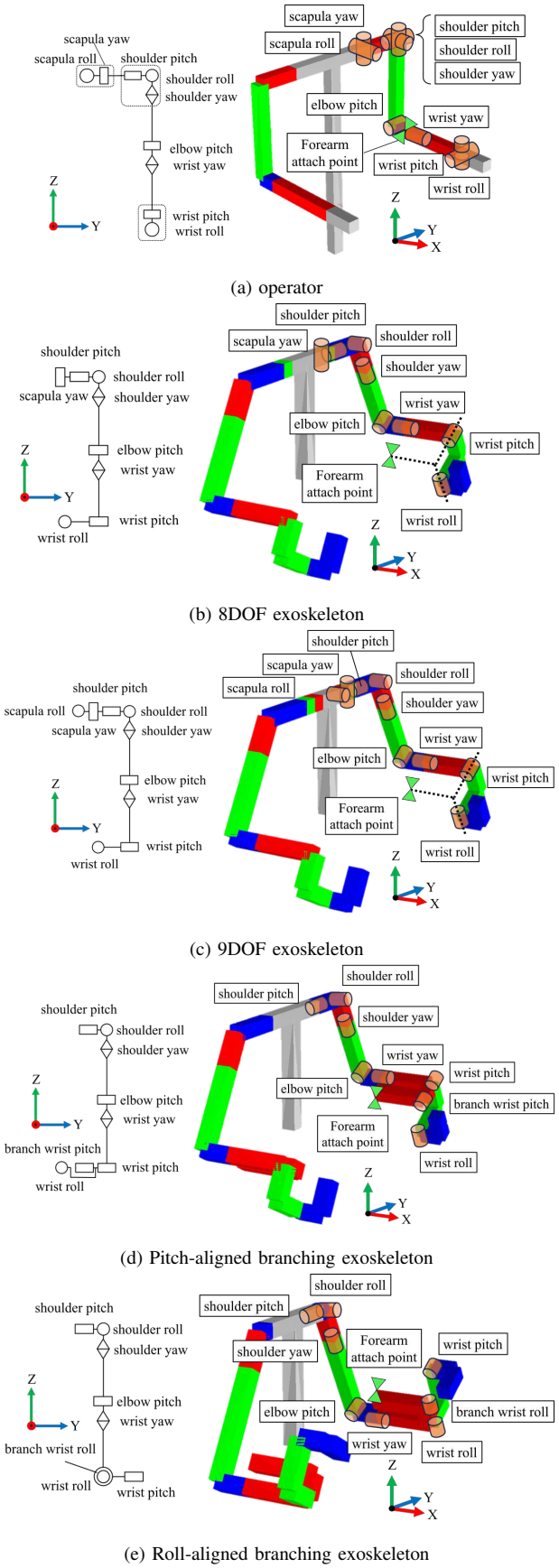

(a) operator

(b) 8DOF exoskeleton

(c) 9DOF exoskeleton

(d) Pitch-aligned branching exoskeleton

(e) Roll-aligned branching exoskeleton

Fig. 5. Simulation models

III. VALIDATION OF BRANCHING EXOSKELETON

In this chapter, the branching exoskeleton is compared and validated against existing exoskeletons based on two key aspects: tracking accuracy with respect to the operator and the required torque.

A. Simulation models

The specific configuration of the branching exoskeleton ensures alignment between the wrist joints of the exoskeleton and those of the operator. This alignment is necessitated by the absence of extra DOFs between the exoskeleton's end-effector and the forearm compared to the operator. Consequently, two potential arrangements exist for each joint, as shown in Fig. 5(d) Pitch-aligned type and (e) Roll-aligned type.In addition to the two branching exoskeleton types, we also modeled and simulated a operator with a 9DOF arm, along with an 8DOF and a 9DOF exoskeleton featuring additional joints on the root link side as shown in Fig. 5(a)(b)(c).

B. Verification of tracking to the operator's forearm

For each exoskeleton, we assumed fixed positions of the end-effector and operator's forearm, and assessed the exoskeleton's ability to track various arm postures of the operator. The procedure to generate the postures of the operator and the exoskeleton was as follows:

1) Set the position and orientation target of the end-effector and generate the operator's posture.
2) Set the target forearm orientation of the operator and determine the operator's posture within the remaining DOFs.
3) Set the exoskeleton's end-effector position and orientation targets with those of the operator's end-effector, and generate the exoskeleton's posture.
4) Set the target position of the exoskeleton's forearms to match the operator's forearm position, and determine the exoskeleton's posture within the remaining DOFs.

The prioritized inverse kinematics solution method within the redundant DOFs utilized the approach outlined by Kanoun et al[22]. The self-interference of the exoskeletons and the interference between the operator and the exoskeleton were not considered through simulations.

In the final stage, if the exoskeleton possesses fewer degrees of freedom than the operator's arms, it may not perfectly align with the operator's forearms. In this study, successful tracking is defined as instances where the positional difference between the forearms is within 1mm. The tracking success rate was computed for each end-effector position by altering the posture of the operator's end-effector and forearms, as specified in stage 1 and 2. The method illustrated in Fig. 6 was employed to adjust the posture of the end-effector and forearm. The end-effector posture was varied from -90 to 90 degrees along each of the roll, pitch, and yaw axes in the world coordinate system. For posture adjustments using redundant DOFs, the posture where the elbow was closest to the floor was used as a reference, and the arm was rotated 0 to 60 degrees around the straight line connecting the shoulder joint and wrist joint.

Fig. 7 and Table I display the tracking success rates of each exoskeleton. The two variants of branching exoskeletons, (c) and (d), outperform the 8-DOF exoskeleton (a), demonstrating tracking efficiency under the 9-DOF exoskeleton (b). However, the actual workspace and range of motion of the operator is smaller than the simulation because of the exoskeleton's self-interference and interference with the operator. Despite being 8-DOF mechanisms, branching exoskeletons consider to be able to accommodate a significant portion of human arm movements.

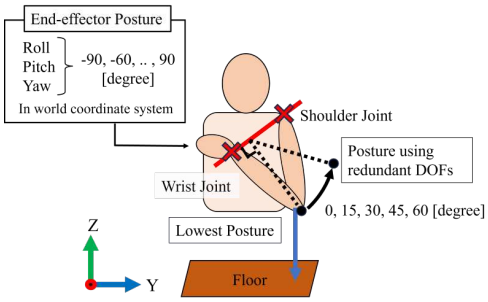

Fig. 6. The method deciding the whole arm posture of the operator

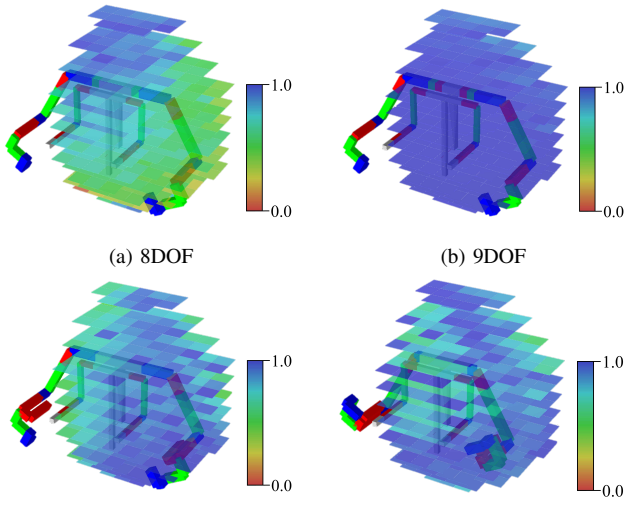

(a) 8DOF (b) 9DOF

(c) Pitch-aligned branching (d) Roll-aligned branching

Fig. 7. The heatmaps of tracking success-rates of exoskeletons to the operator's forearm

TABLE I

THE TRACKING SUCCESS-RATES OF EXOSKELETONS TO THE OPERATOR'S FOREARM

exoskeleton type	mean	median
(a) 8DOF	0.67	0.70
(b) 9DOF	0.99	1.0
(c) Pitch-aligned Branching	0.84	0.86
(d) Roll-aligned Branching	0.87	0.91

C. Verification of torque on additional joints

Using the 7-DOF exoskeleton as a reference, the exoskeleton in Fig. 5 has additional joints. The torque required for these joints is inversely proportional to the compactness of the mechanism. This section compares the torques of these additional joints across the four exoskeleton types in Fig. 5. Initially, the end effectors of the operator and the exoskeleton are attached, as are the operator's and the exoskeleton's forearms. The end-effector's position is set to the operator's initial posture shown in Fig. 5(a), and the operator's arm posture is adjusted using the method in Fig. 6. For each scenario where the exoskeleton applies a force of (10, 0, 0)[N], (0, 10, 0)[N], or (0, 0, 10)[N] to the operator's forearm in the world coordinate system, the average squared torque of each exoskeleton joint is calculated. The results are displayed in Fig. 8. The figure's red bars represent the average squared torques of the additional joints. The torques needed for the two types of branching exoskeleton's additional joints are smaller than those of the 8-DOF and 9-DOF exoskeletons, and are similar to the wrist-yaw joints' torques. Additionally, the sum of the squared torques of all joints is calculated for cases where the force is applied to the operator's end-effector and the forearm, as shown in Fig. 9. This figure shows that the branching exoskeleton requires less overall arm torque. These results suggest that the branching exoskeleton requires small torque to apply force to the operator, making it a low-power mechanism.

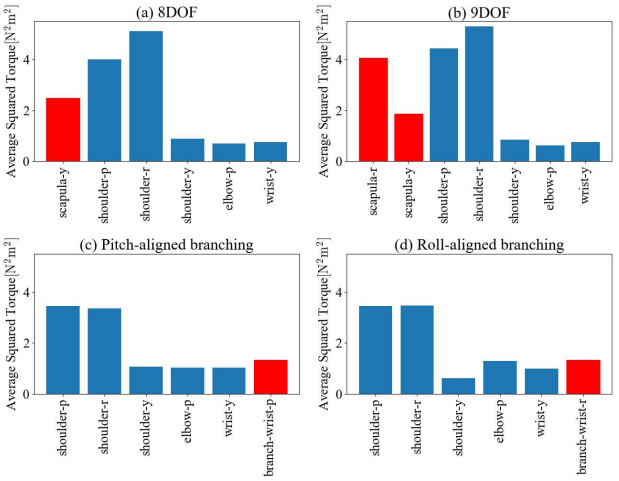

Fig. 8. The average squared torque at each joint of the exoskeletons during various changes in the posture of the operator with the end-effector position fixed at the initial posture. Red bars represent those of additional joints.

IV. MECHANICAL DESIGN

In this study, a pitch-aligned branching exoskeleton was chosen, considering the potential collision between the operator and the exoskeleton, as well as the size of the drive system components. The 7-DOF end-fixed type exoskeleton TABLIS[8] serves as the base, and joint arrangement of the newly designed exoskeleton is depicted in Fig. 10. All motors used are Maxon EC-4pole 200W motors, with output torque adjusted by altering the reduction ratio at each joint.

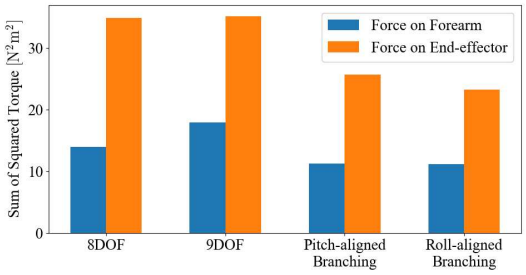

Fig. 9. Sum of the average squared torques at each joint of the exoskeletons for the cases of applying force on the operator's end-effector and on the forearm.

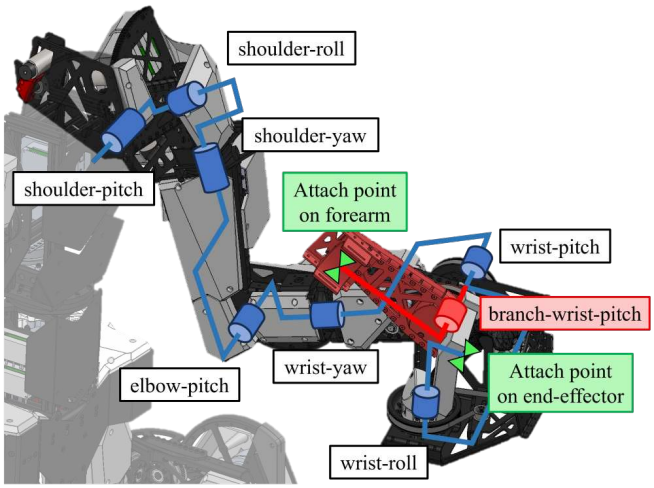

Fig. 10. Arrangement of joints in newly designed branching exoskeleton

Table II shows the nominal torque and no-load speed of each joint. The branch link operates with the same reduction ratio as the wrist joint, factoring in the required torque to apply force discussed in the previous chapter, the self-weight compensation torque, and component placement. Table III lists the mass of each link. All frames are fabricated from sheet metal to minimize weight. The branch link is the second lightest, following the wrist-roll link at the end of the arm.

Fig. 11(a) provides a detailed view of the exoskeleton's wrist section, where the wrist-pitch and branch-wrist-pitch axes align coaxially, and the wrist-roll axis intersects these joint axes. The design positions the operator's wrist joints at these intersections. As depicted in Fig. 11(b), the operator's

TABLE II
NOMINAL CONTINUOUS TORQUE AND NO-LOAD SPEED OF EACH JOINT

Joint	Torque [N m]	speed [rad/s]
shoulder pitch	14.7	12.6
shoulder roll	14.7	12.6
shoulder yaw	9.79	18.9
elbow pitch	9.79	18.9
wrist yaw	5.88	31.6
wrist pitch	4.20	44.2
wrist roll	4.20	44.2
branch wrist pitch	4.20	44.2

grip secures the end-effectors of the exoskeleton and the operator, and a belt attaches the operator's forearm to the branch link. In this research, we designed only the links from the elbow to the end-effector to use TABLIS as a branching exoskeleton. This method can be applied to a standard 7-DOF robot arm to create a branching exoskeleton, demonstrating the branching exoskeleton's effectiveness from a design cost perspective.

TABLE III

MASS OF EACH LINK WITH DRIVE-TRAIN

Link	Mass [kg]
shoulder pitch	1.82
shoulder roll	2.28
shoulder yaw	1.95
elbow pitch	1.71
wrist yaw	1.84
wrist pitch	1.58
wrist roll	0.56
branch	1.44

(a)

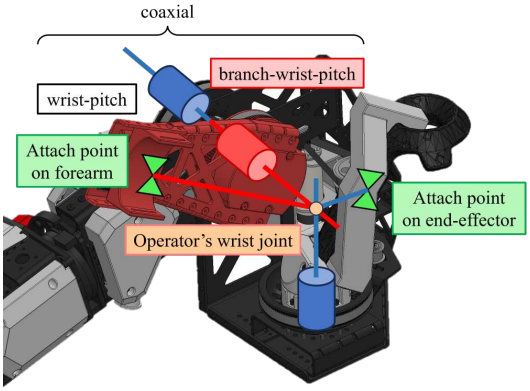

(b)

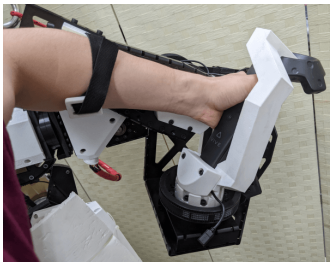

Fig. 11. Closeup of the wrist of the exoskeleton. (a) Arrangement of joints. (b) Operator attaching the exoskeleton

V. EXPERIMENTS

The exoskeleton was linked to the robot to execute arm movements, including redundant DOFs. We utilized JAXON[23], a robot with 8-DOFs in its arms. Upon connecting the robot and the exoskeleton, the initial values were set for the position and posture of the operator's end-effector and the posture of the forearms. The robot received the differences from these initial values. For the end-effector, all 6-DOFs were exchanged. However, for the forearm, only the direction from the elbow to the wrist was crucial, leading to the use of 2-DOFs, excluding the roll axis. The robot solved inverse kinematics to generate a standing posture under these 8-DOFs constraints.

(a)

(b)

(c)

Fig. 12. Operating an actual humanoid performing a movement requring forearm posture. (a) Sliding the tray on the desk around a glass. (b) Resting a shopping basket on the elbow. (c) Tucking a cylindrical object under the arm.

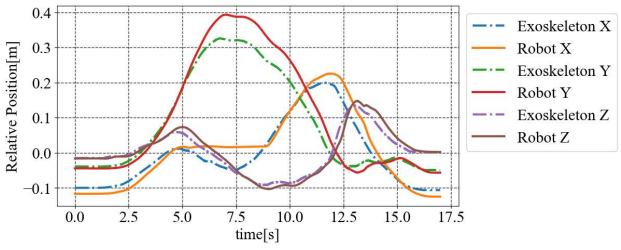

(a) End-effector Position

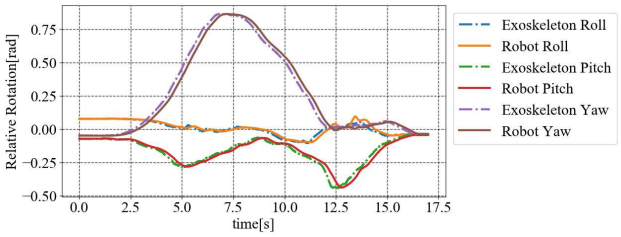

(b) End-effector Rotation

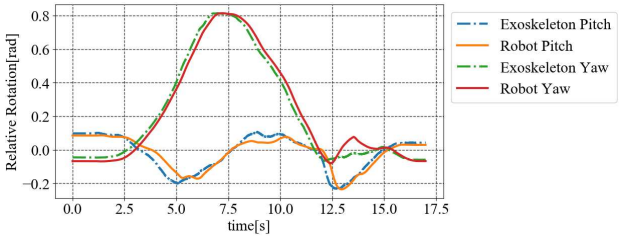

(c) Forearm Rotation

Fig. 13. Relative position and rotation from initial posture between the operator and the command from exoskeleton at their end-effectors and forearms

As depicted in Fig. 12, three critical movements were executed that required forearm posture control: sliding the tray on the desk around a glass, resting a shopping basket on the elbow, and tucking a cylindrical object under the arm. Fig. 13 illustrates the alterations in the end-effector's position and orientation, as well as the forearms' posture, relative to the operator and the robot during the tray sliding motion. These changes in position and posture are represented in the world coordinate system. Fig. 13 demonstrates that the robot closely follows commands for both the end-effector and forearm postures. However, after approximately 5 seconds, the end-effector position deviates from the commanded value. This deviation is likely due to the robot adjusting its commands to prevent self-interference as the arm approaches the torso. Consequently, the robot adjusts its movements gradually to avoid sudden changes between the commanded and actual postures. The robot's adherence to the operator's commands demonstrates its ability to execute movements using its forearms, facilitated by the branching exoskeleton.

VI. CONCLUSIONS

In this study, we have proposed a novel type exoskeleton for humanoid robot arm manipulation, named "branching exoskeleton". This exoskeleton is characterized by the utilization of the branched link attaching the operator's forearm to itself. Despite this exoskeleton has 8-DOFs on its arm, its tracking performance to the operator is superior to an exoskeleton with traditional 8-DOF structure.By adding an extra link to attach the operator's forearm on the end-effector side, minimal torque and low power consumption are achieved. This branching type exoskeleton has illustrated the capability to manage the redundant DOFs of a actual humanoid robot. Our exoskeleton can make contributions to research on platforms for robot manipulation.

REFERENCES

[1] Kourosh Darvish, et al. Teleoperation of humanoid robots: A survey. *IEEE Trans. Robot.*, Vol. 39, No. 3, pp. 1–22, 2023.

[2] D Haering, M Raison, and M Begon. Measurement and description of three-dimensional shoulder range of motion with degrees of freedom interactions. *J. Biomech. Eng.*, Vol. 136, No. 8, August 2014.

[3] Yves Zimmermann, Michael Sommerhalder, Peter Wolf, Robert Riener, and Marco Hutter. ANYexo 2.0: A fully actuated Upper-Limb exoskeleton for manipulation and Joint-Oriented training in all stages of rehabilitation. *IEEE Trans. Rob.*, Vol. 39, No. 3, pp. 2131–2150, June 2023.

[4] B Kim and A D Deshpande. An upper-body rehabilitation exoskeleton harmony with an anatomical shoulder mechanism: Design, modeling, control, and performance evaluation. *Int. J. Rob. Res.*, Vol. 36, No. 4, pp. 414–435, April 2017.

[5] Yuansheng Ning, et al. An eight-degree-of-freedom upper extremity exoskeleton rehabilitation robot: design, optimization, and validation. *J. Mech. Sci. Technol.*, Vol. 36, No. 11, pp. 5721–5733, November 2022.

[8] Yasuhiro Ishiguro, et al. Bilateral humanoid teleoperation system using Whole-Body exoskeleton cockpit TABLIS. *IEEE Robotics and Automation Letters*, Vol. 5, No. 4, pp. 6419–6426, October 2020.

[6] Thomas Hulin, et al. The DLR bimanual haptic device with optimized workspace. In *2011 IEEE International Conference on Robotics and Automation*, pp. 3441–3442, May 2011.

[7] C Zhou, L Zhao, H Wang, L Chen, and Y Zheng. A bilateral Dual-Arm teleoperation robot system with a unified control architecture. In *2021 30th IEEE International Conference on Robot & Human Interactive Communication (RO-MAN)*, pp. 495–502, August 2021.

[9] A Wang, J Ramos, J Mayo, W Ubellacker, J Cheung, and S Kim. The HERMES humanoid system: A platform for full-body teleoperation with balance feedback. In *2015 IEEE-RAS 15th International Conference on Humanoid Robots (Humanoids)*, pp. 730–737, November 2015.

[10] M H Rahman, M J Rahman, O L Cristobal, M Saad, J P Kenné, and P S Archambault. Development of a whole arm wearable robotic exoskeleton for rehabilitation and to assist upper limb movements. *Robotica*, Vol. 33, No. 1, pp. 19–39, January 2015.

[11] F Falck, K Larppichet, and P Kormushev. DE VITO: A Dual-Arm, high Degree-of-Freedom, lightweight, inexpensive, passive Upper-Limb exoskeleton for robot teleoperation. In *Towards Autonomous Robotic Systems*, pp. 78–89. Springer International Publishing, 2019.

[12] P. Letier, et al. Sam : A 7-dof portable arm exoskeleton with local joint control. In *2008 IEEE/RSJ International Conference on Intelligent Robots and Systems*, pp. 3501–3506, 2008.

[13] R A R C Gopura, K Kiguchi, and Y Li. SUEFUL-7: A 7DOF upper-limb exoskeleton robot with muscle-model-oriented EMG-based control. In *2009 IEEE/RSJ International Conference on Intelligent Robots and Systems*, pp. 1126–1131, October 2009.

[14] Yupeng Ren, Hyung-Soon Park, and Li-Qun Zhang. Developing a whole-arm exoskeleton robot with hand opening and closing mechanism for upper limb stroke rehabilitation. In *2009 IEEE International Conference on Rehabilitation Robotics*, pp. 761–765. IEEE, June 2009.

[15] Manbok Hong, Sin Jung Kim, and Keehoon Kim. KULEX: ADL power assistant robotic system for the elderly and the disabled (abstract for video). In *2013 10th International Conference on Ubiquitous Robots and Ambient Intelligence (URAI)*, pp. 121–122. IEEE, October 2013.

[16] T Nef, M Guidali, and R Riener. ARMin III –arm therapy exoskeleton with an ergonomic shoulder actuation. *Appl. Bionics Biomech.*, Vol. 6, pp. 127–142, April 2009.

[17] Sung-Hua Chen, et al. Assistive control system for upper limb rehabilitation robot. *IEEE Trans. Neural Syst. Rehabil. Eng.*, Vol. 24, No. 11, pp. 1199–1209, November 2016.

[18] Urs Keller, Hubertus J A van Hedel, Verena Klamroth-Marganska, and Robert Riener. ChARMin: The first actuated exoskeleton robot for pediatric arm rehabilitation. *IEEE/ASME Trans. Mechatron.*, Vol. 21, No. 5, pp. 2201–2213, October 2016.

[19] Lorenzo Grazi, Emilio Trigili, Giulio Proface, Francesco Giovacchini, Simona Crea, and Nicola Vitiello. Design and experimental evaluation of a semi-passive upper-limb exoskeleton for workers with motorized tuning of assistance. *IEEE Trans. Neural Syst. Rehabil. Eng.*, Vol. 28, No. 10, pp. 2276–2285, October 2020.

[20] Jun Pan, et al. NESM-γ: An Upper-Limb exoskeleton with compliant actuators for clinical deployment. *IEEE Robotics and Automation Letters*, Vol. 7, No. 3, pp. 7708–7715, July 2022.

[21] Amin Zeiaee, Rana Soltani Zarrin, Andrew Eib, Reza Langari, and Reza Tafreshi. CLEVERarm: A lightweight and compact exoskeleton for upper-limb rehabilitation. *IEEE Robot. Autom. Lett.*, Vol. 7, No. 2, pp. 1880–1887, April 2022.

[22] O Kanoun, F Lamiraux, PB Wieber, F Kanehiro, E Yoshida, and JP Laumond. Prioritizing linear equality and inequality systems: Application to local motion planning for redundant robots. In *2009 IEEE International Conference on Robotics and Automation*, pp. 2939–2944, May 2009.

[23] Kunio Kojima, et al. Development of life-sized high-power humanoid robot JAXON for real-world use. In *2015 IEEE-RAS 15th International Conference on Humanoid Robots (Humanoids)*, pp. 838–843. ieeexplore.ieee.org, November 2015.